Generalized theory of diffusion based on kinetic theory

T. Schäfer
Department of Physics, North Carolina State University, Raleigh, North Carolina 27695, USA
(Received 12 September 2016; published 26 October 2016)

We propose to use spin hydrodynamics, a two-fluid model of spin propagation, as a generalization of the diffusion equation. We show that in the dense limit spin hydrodynamics reduces to Fick's law and the diffusion equation. In the opposite limit spin hydrodynamics is equivalent to a collisionless Boltzmann treatment of spin propagation. Spin hydrodynamics avoids unphysical effects that arise when the diffusion equation is used to describe to a strongly interacting gas with a dilute corona. We apply spin hydrodynamics to the problem of spin diffusion in a trapped atomic gas. We find that the observed spin relaxation rate in the high-temperature limit [Sommer *et al.*, Nature (London) **472**, 201 (2011)] is consistent with the diffusion constant predicted by kinetic theory.

DOI: 10.1103/PhysRevA.94.043644

I. INTRODUCTION

Diffusion plays an important role in many areas of physics, and the problem of finding numerical and analytical solutions to the diffusion equation is well understood [1]. However, many interesting applications of the diffusion equation involve problems in which the mean-free path varies significantly, so that the diffusion approximation breaks down in the dilute, weakly collisional regime. In this case a naive treatment of the diffusion equation will lead to unphysical results. In a dilute gas the diffusion coefficient scales inversely with the density, and the diffusion current can become unphysically large. This problem can be dealt with in a phenomenological way by using flux limiters or boundary conditions. However, given that the dilute regime is physically well understood, it should be possible to derive quantitatively accurate schemes that interpolate between diffusion and ballistic motion.

In this work we propose a generalization of the diffusion equations that correctly extrapolates to the ballistic limit. The method is based on moments of the Boltzmann equation, and bears some resemblance to moment methods employed for radiation hydrodynamics in astrophysics [2,3]. The method was inspired by recent work on anisotropic fluid dynamics, which has been used to implement the correct ballistic limit of the Navier-Stokes equation in relativistic and nonrelativistic fluid dynamics [4–7] (see Ref. [8] for a different approach to this problem, based on the lattice Boltzmann method).

The work was motivated by attempts to extract the spin diffusion constant of ultracold atomic gases from experiments with optically trapped atoms [9–11], see also Refs. [12–15]. A particularly interesting system is the two-component unitary Fermi gas. In this case the two-body scattering length is infinite, and the diffusion constant is expected to enter the quantum regime $D \sim \hbar/m$, where m is the mass of the particles [16]. The determination of the spin diffusion constant from experiment is in principle straightforward. The experiment involves preparing a 50-50 mixture of spin-up and spin-down particles. The two spin components are spatially separated and then released. The early time dynamics is typically complicated, but at late times exponential relaxation to a locally balanced mixture is observed. The diffusion constant depends on the local density n and temperature T, but this dependence can be unfolded by performing experiments at different temperatures, and for different numbers of particles. In the unitary Fermi gas the situation is further simplified by scale invariance, which implies that $D = \frac{\hbar}{m} f(mTn^{-2/3})$ where $f(x)$ is a function of a single variable.

The tool for extracting the diffusion constant is the diffusion equation. We have to construct solutions of the diffusion equation in a given trap geometry and adjust the diffusion constant in order to achieve agreement with the observed spin relaxation times. The difficulty, as pointed out in the present context by Bruun and Pethick [17], is that the diffusion approximation breaks down in the dilute part of the cloud. If this issue is ignored, observed spin relaxation times disagree with theoretical expectations by more than an order of magnitude. Bruun and Pethick proposed to address this issue by imposing a transverse cutoff on the diffusion equation in an elongated trap. The cutoff radius is determined by a simple mean-free path estimate, or fitted to experiment. A similar procedure for estimating shear viscosity was used in Ref. [18].

In the present work we propose to improve on this procedure by deriving a generalization of the diffusion equation, which we call spin hydrodynamics. Spin hydrodynamics describes the transition from diffusive to ballistic behavior dynamically, based on a relaxation time equation. The paper is structured as follows. In Sec. II we review the derivation of Fick's law from kinetic theory, and in Sec. III we discuss the behavior of variational and numeric solutions of the diffusion equation in a harmonically trapped gas. The equations of spin fluid dynamics are derived in Sec. IV, and the diffusive and ballistic limits are studied in Sec. V. A numerical method for implementing spin hydrodynamics is described in Sec. VI. Numerical tests are presented in Sec. VII, and numerical results in a trap geometry are given in Sec. VIII. We provide an outlook in Sec. IX.

II. KINETIC THEORY AND DIFFUSION EQUATION

In this section we review the derivation of the spin diffusion equation from kinetic theory in a two-component Fermi gas. Consider the Boltzmann equation

$$(\partial_0 + \vec{v}\cdot\vec{\nabla}_x + \vec{F}\cdot\vec{\nabla}_p) f_{p\sigma}(x,t) = C[f_{p\sigma}], \qquad (1)$$

where $f_{p\sigma}(x,t)$ is the phase space density of particles with spin $\sigma = \uparrow\downarrow$, $\vec{v}$ is the velocity of the particles, $\vec{F}$ is a force, and $C[f_{p\sigma}]$ is the collision term. For quasiparticles with energy E_p we have

$$\vec{v} = \vec{\nabla}_p E_p, \quad \vec{F} = -\vec{\nabla}_x E_p. \tag{2}$$

We will focus on the case $E_p = \epsilon_p + V(x)$, where ϵ_p is solely a function of momentum, and $V(x)$ is an external spin-independent potential. We are interested in the spin current $\vec{j}_M = \vec{j}_\uparrow - \vec{j}_\downarrow$ generated in response to a magnetization gradient $\vec{\nabla} M$, where $M = n_\uparrow - n_\downarrow$. Here, the spin densities and currents are given by

$$n_\sigma(x,t) = \int d\Gamma\, f_{p\sigma}(x,t), \quad \vec{j}_\sigma(x,t) = \int d\Gamma\, \vec{v}\, f_{p\sigma}(x,t), \tag{3}$$

where $d\Gamma = d^3p/(2\pi)^3$. If the collision term conserves spin then the Boltzmann equation implies

$$\partial_0 M + \vec{\nabla}\cdot\vec{j}_M = 0. \tag{4}$$

We will focus on near-equilibrium distributions of the form

$$f_{p\sigma}(x,t) = f^0_{p\sigma}(x,t)\left(1 + \frac{\chi_{p\sigma}(x,t)}{T}\right), \tag{5}$$

$$f^0_{p\sigma}(x,t) = \exp\left(-\frac{1}{T(x,t)}[\epsilon_p + V(x) - \mu_\sigma(x,t)]\right). \tag{6}$$

For simplicity we make the relaxation time [Bhatnagar-Gross-Krook (BGK)] approximation to the collision term

$$C[f_{p\sigma}] = -\frac{f^0_{p\sigma}\chi_{p\sigma}}{T\tau}, \tag{7}$$

where τ is a collision time. It is straightforward to solve the Boltzmann equation at leading order in τ and in gradients of the thermodynamic variables. We find

$$\chi_{\sigma p} = -\tau\vec{v}\cdot\vec{\nabla}\mu_\sigma \tag{8}$$

and

$$\vec{j}_M = -D_\mu\vec{\nabla}\delta\mu, \quad D_\mu = \frac{\tau}{3T}\int d\Gamma\, v^2 f^0_p, \tag{9}$$

where $\delta\mu = \mu_\uparrow - \mu_\downarrow$. For $\epsilon_p = p^2/(2m)$ we get $D_\mu = (\tau n)/(2m)$. Finally, we obtain the standard form of Fick's law by changing variables from $\delta\mu$ to M,

$$\vec{j}_M = -D[\vec{\nabla}M - k_n\vec{\nabla}n], \quad D = \chi_M^{-1}D_\mu, \tag{10}$$

where $\chi_M = (\partial M)/(\partial\delta\mu)$ and $k_n = \chi_n/\chi_M$ with $\chi_n = (\partial n)/(\partial\delta\mu)$. For a noninteracting gas $\chi_M = n/(2T), k_n = M/n$, and $D = (\tau T)/m$. Note that D has units $\hbar/m$, and the quantum limit corresponds to $\tau = \hbar/T$. In the following we will set $\hbar = k_B = 1$. For a given collision term we can express the collision time τ in terms of the scattering parameters. In the dilute Fermi gas at unitarity we have $\sigma = 4\pi/k^2$ where k is the relative momentum of the spin up and down particles. Solving the Boltzmann equation at leading order in gradients gives [9,16]

$$D = \frac{9\pi^{3/2}}{32\sqrt{2}m}\left(\frac{T}{T_F}\right)^{3/2}, \tag{11}$$

where $T_F = k_F^2/(2m)$ is the Fermi temperature, and $k_F = (3\pi^2 n)^{1/3}$ is the Fermi momentum. The result in Eq. (11) was obtained at leading order in an expansion of $\chi_{\sigma p}$ in Laguerre polynomials. The next order correction has not been computed, but the corresponding approximation is known to be accurate to better than 2% for other transport coefficients, such as the shear viscosity. The most important feature of Eq. (11) is that $D \sim 1/n$, which is a general result that follows from kinetic theory in the dilute limit. More detailed studies of spin diffusion were performed by Enss and collaborators [19–22].

III. DIFFUSION IN THE HIGH- AND LOW-TEMPERATURE LIMITS

Solutions to the diffusion equation is a trapped atomic system were studied by Bruun and Pethick [17]. Here we will briefly review their study, and generalize the result to low-temperature gases. We consider the diffusion equation, Eqs. (4) and (10). We will assume $k_n = M/n$, so that the diffusion equation takes a simple form when written in terms of the polarization $P = M/n$. We find

$$\partial_0 P - \frac{1}{n}\vec{\nabla}[nD\,\vec{\nabla}P] = 0. \tag{12}$$

We are interested in solutions of the form $P(x,t) = e^{-\Gamma_i t}P_i(x)$. In the asymptotic limit the solution is dominated by the lowest mode $\Gamma \equiv \Gamma_0$. This equation further simplifies in the high-temperature limit where $nD = \text{const}$. In that case the diffusion equation is

$$\partial_0 P - \frac{n(0)D(0)}{n}\nabla^2 P = 0, \tag{13}$$

where $n(0)$ and $D(0)$ are the density and diffusion constant at the trap center. Bruun and Pethick observed that this equation can be solved using variational methods, in analogy to the Schrödinger equation. The variational bound on Γ is

$$\Gamma \leqslant n(0)D(0)\,\frac{\int d^3x\,[\vec{\nabla}P_v(x)]^2}{\int d^3x\, n(x)P_v(x)^2}, \tag{14}$$

where $P_v(x)$ is a variational function. Consider a dilute Fermi gas in a harmonic trapping potential $V(x) = \frac{1}{2}m\omega_i^2 x_i^2$. In that case $n(x) = n(0)\exp[-V(x)/T]$. We will focus on axially symmetric potentials $\omega_x = \omega_y \equiv \omega_\perp$ and $\omega_z = \lambda\omega_\perp$. On dimensional grounds we have

$$\Gamma = \frac{D(0)}{l_z^2}\Gamma_{\rm red}(\lambda), \tag{15}$$

where $l_z^2 = 2T/(m\omega_z^2)$ is the square of the oscillator length in the z direction, and $\Gamma_{\rm red}$ is a dimensionless damping constant. A variational ansatz with the correct symmetry and asymptotic behavior is

$$P_v(x) = \frac{z}{1+\tilde{R}^3}, \quad \tilde{R} = \left(\frac{x^2+y^2}{d_\rho^2} + \frac{z^2}{d_z^2}\right)^{1/2}, \tag{16}$$

where d_ρ and d_z are variational parameters. Using this ansatz we find $\Gamma_{\rm red}(\lambda{=}0) = 12.1, \Gamma_{\rm red}(\lambda{=}0.4) = 29.2$ and $\Gamma_{\rm red}(\lambda\to 0) = \lambda^{-2}/\ln(0.13\lambda^{-2})$. The limit $\lambda \to 0$ can be derived rigorously using a WKB approximation.

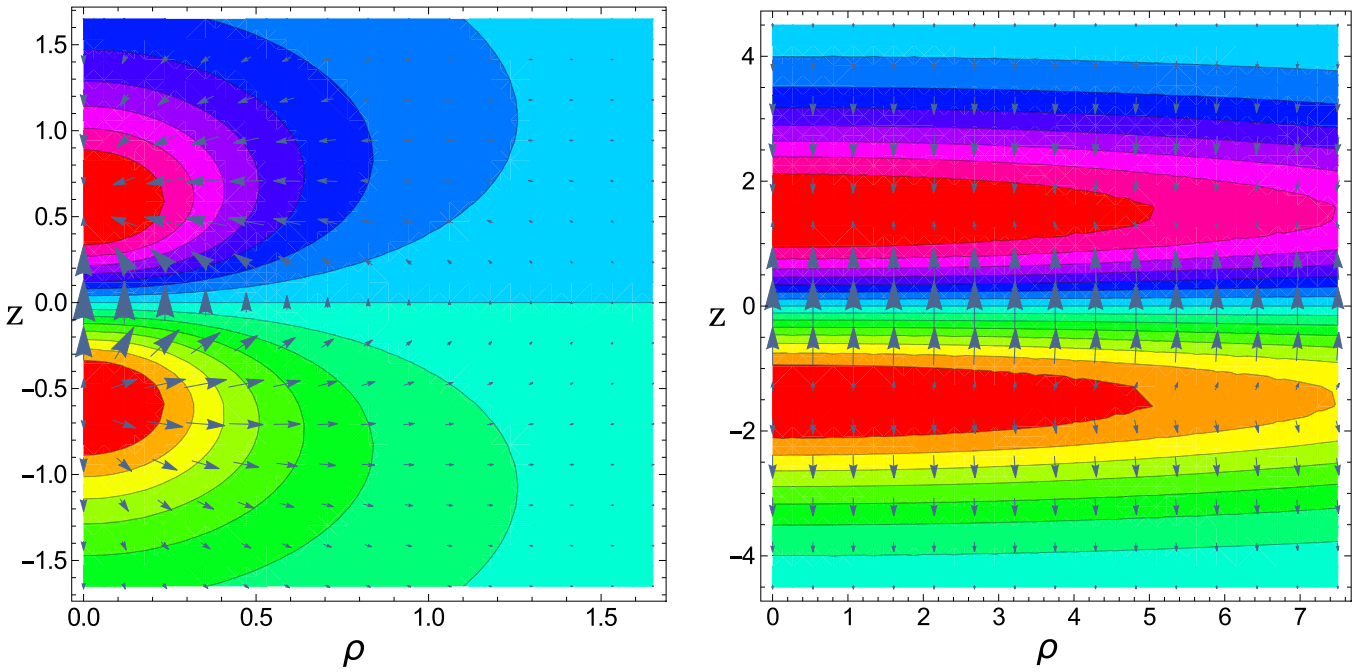

FIG. 1. Solutions of the spin diffusion equation for a gas confined in a harmonic potential with deformation $\lambda = 0.4$. The contours show the polarization P as a function of the dimensionless variables $\bar{\rho}$ and $\bar{z}$, and the vector field shows the spin current $\vec{j}$. The contour plots have 15 equally spaced contour lines between the maximum and minimum polarization at the center of the trap. The left panel shows a solution in the high-temperature limit $D = D(0)n(0)/n$, and the right panel corresponds to the low-temperature limit $D = D(0)$.

The experimental work reports the spin drag coefficient $\Gamma_{sd} = \omega_z^2/\Gamma$ in units of the Fermi Energy $E_F(0)$. Note that $E_F(0)$ refers to the local Fermi energy at the trap center. The result is based on the observed decay rate of the spin dipole moment. In the high-temperature limit Sommer *et al.* find $\Gamma_{sd} = 0.16\, E_F(0)(T_F/T)^{1/2}$ [9]. The experimental paper does not provide the value of λ, but states that in the regime that was investigated the spin drag $\Gamma_{sd}/E_F(0)$ is independent of λ. Using Eqs. (11) and (15) we obtain the theoretical prediction

$$\Gamma_{sd} = \frac{1.81\, E_F(0)}{\Gamma_{\rm red}(\lambda)} \left(\frac{T_F}{T}\right)^{1/2}. \tag{17}$$

For a strongly deformed cloud $\Gamma_{\rm red} \gtrsim \Gamma_{\rm red}(0.1) \simeq 200$, which differs from the experimental result $\Gamma_{\rm red} \simeq 11.3$ by more than an order of magnitude. Bruun and Pethick argued that the discrepancy is related to the treatment of the dilute part of the cloud, and suggested imposing a transverse cutoff r_0 in Eq. (14). The result is very sensitive to the precise value of r_0, but the experimental result can be understood for a reasonable value $r_0 = 2.1 l_\perp$, where $l_\perp$ is the transverse oscillator length.

For comparison we have studied diffusion in a low-temperature gas. Here, we assume that the low-temperature limit corresponds to $D = D(0)$, which means that the diffusion constant is only a function of temperature and not of density. This is a slight idealization, because in a degenerate Fermi gas the diffusion constant is expected to exhibit the Landau Fermi liquid behavior $mD \sim (T_F/T)^2$ [16]. Combined with Eq. (11) this result implies that mD has a minimum as a function of T/T_F, and that near the minimum there is a regime in which the diffusion constant is approximately density independent. In this limit the diffusion equation is

$$\partial_0 P - \frac{D(0)}{n} \vec{\nabla}[n \vec{\nabla} P] = 0. \tag{18}$$

The variational principle gives

$$\Gamma \leqslant D(0) \frac{\int d^3x\, n(x) [\vec{\nabla} P_v(x)]^2}{\int d^3x\, n(x) P_v(x)^2}. \tag{19}$$

This equation is minimized by $\Gamma_{\rm red} = 2$ and $P_v(x) \sim z$, independent of λ. The result that $\Gamma_{\rm red}$ is approximately λ independent is consistent with experiment, but the value of $\Gamma_{\rm red}$ is not. Whereas the value $\Gamma_{\rm red}$ in the dilute limit is too large, the value in the dense limit is too small. This suggest that the correct spin current profile must be intermediate between the structure in the high- and low-temperature limits.

In order to verify the variational estimates we have numerically solved the diffusion equation in the high- and low-temperature limits. In the high-temperature limit we assume that $D = D(0)n(0)/n$. The diffusion equation in cylindrical coordinates is

$$\partial_{\bar{t}} P - e^{-\bar{V}} \left[\frac{1}{\bar{\rho}} \partial_{\bar{\rho}} (\bar{\rho} \partial_{\bar{\rho}} P) + \partial_{\bar{z}}^2 P\right] = 0, \tag{20}$$

where $\bar{\rho} = (x^2 + y^2)^{1/2}/l_z$ and $\bar{z} = z/l_z$ are dimensionless variables and $\bar{V} = \lambda^{-2}\bar{\rho}^2 + \bar{z}^2$. The dimensionless time variable is $\bar{t} = m\omega_z^2 D(0) t/(2T)$, so that Γ is automatically given in units of $D(0)/l_z^2$. A solution of the diffusion equation for $\lambda = 0.4$ is shown in Fig. 1. The decay constant of the spin current is $\Gamma_{\rm red} \simeq 29$, which agrees with the variational estimate $\Gamma_{\rm red} = 29.2$. It is important to note that the spin current is not quasi-one-dimensional, even in a deformed trap.

Using cylindrical coordinates the diffusion equation in the dense limit is given by

$$\partial_{\bar{t}} P - \left[\partial_{\bar{\rho}}^2 + \frac{1}{\bar{\rho}}\partial_{\bar{\rho}} + \partial_{\bar{z}}^2 - 2\left(\bar{z}\partial_{\bar{z}} + \frac{\bar{\rho}}{\lambda^2}\partial_{\bar{\rho}}\right)\right] P = 0. \quad (21)$$

A solution of the diffusion equation is shown in the right panel of Fig. 1. We observe that the distribution of spin current is very different from the dilute limit. In particular, we find that diffusion is approximately one dimensional. The decay constant is $\Gamma_{\rm red} \simeq 2$, in very good agreement with the variational estimate. This result implies that the decay of the magnetization is much slower (by almost a factor 15) as compared to the dilute limit. This result is easy to understand: In the dilute regime spin polarization decays by generating a large spin current in the dilute corona. In the dense limit the polarization has to decay by producing much smaller currents in the dense part of the cloud.

IV. SPIN HYDRODYNAMICS AND KINETIC THEORY

In order to improve the accuracy of the diffusion equation in the dilute limit we revisit the derivation of the diffusion equation in kinetic theory. Consider the Boltzmann transport equation, Eq. (1), with a two-body collision term

$$C[f_{p_1\sigma_1}] = \sum_{\sigma_2\sigma_3\sigma_4}\int d\Gamma_{234}\left(f_{p_1\sigma_1}f_{p_2\sigma_2} - f_{p_3\sigma_3}f_{p_4\sigma_4}\right) \times w(p_1\sigma_1, p_2\sigma_2; p_3\sigma_3, p_4\sigma_4), \quad (22)$$

where w is the transition amplitude. We assume that w is of the form

$$w(p_1\sigma_1, p_2\sigma_2; p_3\sigma_3, p_4\sigma_4) = (2\pi)^4\delta\left(\sum_i E_i\right)\delta\left(\sum_i p_i\right)\delta_{\sigma_1+\sigma_2,\sigma_3+\sigma_4}| \times \mathcal{A}_{\sigma_1\sigma_2}(P,q)|^2, \quad (23)$$

where $2P = p_1 + p_2$ and $2q = p_1 - p_2$. In this case moments of the collision operator with respect to particle number, momentum, and energy vanish

$$\sum_\sigma \int d\Gamma\, R_i(p) C[f_{p\sigma}] = 0, \quad (24)$$

where $R_i = \{1, \vec{p}, \epsilon_p\}$. Similarly, conservation of spin implies

$$\sum_\sigma \int d\Gamma\, \bar{\sigma} C[f_{p\sigma}] = 0, \quad (25)$$

where $\bar{\sigma} = \pm$ for $\sigma = \uparrow, \downarrow$. This relation does not generalize to other moments such as $\bar{\sigma}\,\vec{p}$ and $\bar{\sigma}\epsilon_p$. The Boltzmann equation and Eq. (24) imply conservation laws for particle number, momentum, and energy

$$\partial_0 n + \vec{\nabla}\cdot\vec{j}_n = 0, \quad (26)$$

$$\partial_0 \pi^i + \vec{\nabla}_j \Pi^{ij} = 0, \quad (27)$$

$$\partial_0 \mathcal{E} + \vec{\nabla}\cdot\vec{j}_\epsilon = 0. \quad (28)$$

Here, $n = n_\uparrow + n_\downarrow, \vec{j}_n = \vec{j}_\uparrow + \vec{j}_\downarrow$ and $\vec{\pi} = m\vec{j}_n$. We also have

$$\Pi_{ij} = \sum_\sigma \int d\Gamma\, f_{\sigma p}\, p_i v_j, \quad (29)$$

$$\mathcal{E} = \sum_\sigma \int d\Gamma\, f_{\sigma p}\, \epsilon_p, \quad (30)$$

$$\vec{j}_\epsilon = \sum_\sigma \int d\Gamma\, f_{\sigma p}\, \vec{v}\,\epsilon_p. \quad (31)$$

Equation (25) implies the spin conservation equation (4). In order to derive the diffusion equation we need a constitutive equation for the spin current $\vec{j}_M$. As shown in Sec. II Fick's law $\vec{j}_M = -D\vec{\nabla}M$ can be derived by assuming that $f_{p\sigma}$ is close to the equilibrium distribution, see Eq. (5). In this section we will follow a different strategy. We derive an equation of motion for $\vec{j}_\sigma$ from the $\vec{p}$ moment of the Boltzmann equation for each σ. We find

$$\partial_0\left(m j_\sigma^i\right) + \vec{\nabla}_j \Pi_\sigma^{ij} - F^i n_\sigma = \int d\Gamma\, p^i\, C[f_{p\sigma}]. \quad (32)$$

In order for the equations of motion to close we need a constitutive equation for the spin stress Π_σ^{ij}, and an explicit expression for the collision term. We will make a generalized ansatz for the distribution function

$$f_{p\sigma}(x,t) = \exp\left(\frac{1}{T(x,t)}\left\{\mu_\sigma(x,t) - \frac{1}{2m}\left[p^i - m u_\sigma^i(x,t)\right]^2\right\}\right), \quad (33)$$

where $\vec{u}_\sigma$ is a spin velocity. Note that this distribution functions includes the Chapman-Enskog ansatz in Eqs. (5) and (8) as a special case. If $\vec{w} = \frac{1}{2}(\vec{u}_\uparrow - \vec{u}_\downarrow)$ is small we can expand Eq. (33) and obtain

$$f_{p\sigma}(x,t) \simeq f_{p\sigma}^0(x,t)\left(1 \pm \frac{m}{T}\vec{v}\cdot\vec{w}\right), \quad (34)$$

where the $\pm$ sign corresponds to $\sigma = \uparrow\downarrow$. We observe that Eq. (8) is recovered for $m\vec{w} = -\frac{\tau}{2}\vec{\nabla}\delta\mu$. However, if $\vec{w}$ is large then $f_{p\sigma}$ is not close to equilibrium. We will show below that Eq. (33) solves the Boltzmann equation in the ballistic limit, and in this way provides a smooth connection between the diffusive and ballistic limits.

We can now derive equations of motion by taking moments of the Boltzmann equation with respect to particle number and momentum for fixed spin. Moments with respect to particle number give the continuity equations

$$\partial_0 n_\sigma + \vec{\nabla}\cdot(n_\sigma\vec{u}_\sigma) = 0. \quad (35)$$

Moments with $\vec{p}$ give equations of motion for $n_\sigma\vec{u}_\sigma$. We get

$$\partial_0\left(m n_\sigma u_\sigma^i\right) + \vec{\nabla}_j \Pi_\sigma^{ij} + n_\sigma F^i = S_\sigma, \quad (36)$$

where F^i is an external force and we have defined the spin stresses

$$\Pi_\sigma^{ij} = m n_\sigma u_\sigma^i u_\sigma^j + n_\sigma T\delta^{ij}. \quad (37)$$

The source term S_σ depends on the collision term. In the BGK approximation

$$C[f_{p\sigma}] = -\frac{f_{p\sigma} - f_{p\sigma}^0}{\tau}, \quad (38)$$

where $f^0_{p\sigma}$ is given in Eq. (6) we obtain $S_\sigma = \mp(mn_\sigma w^i)/\tau$. This result exhibits some unphysical features, related to shortcomings of the BGK approximation. In particular, S_σ does not conserve the total momentum of spin-up and spin-down particles, even though the microscopic collision term in Eq. (22) conserves momentum. We address this problem by replacing $n_\sigma \to n_g$, where $n_g = n_\uparrow n_\downarrow/(n_\uparrow + n_\downarrow)$ is the geometric mean of the up and down densities. This gives

$$S_\sigma = \mp\frac{mn_g w^i}{\tau}. \tag{39}$$

Like the BGK collision term, this is a model for collisional relaxation in a two-component gas. It does, however, have two advantages compared to the BGK model: (i) It conserves total momentum; (ii) The collision rate goes to zero if either one of the two densities goes to zero, as predicted by the full collision term. We note that the collision term is characterized by a single parameter τ, which may depend on n and T. In the following section we will show that in order to reproduce the diffusion equation with diffusion constant $D(n,T)$ the relaxation time should be chosen as

$$\tau(T,n) = \frac{mD(n,T)}{T}. \tag{40}$$

In a weakly polarized gas ($n_\uparrow \simeq n_\downarrow$) this is the same relation we obtained from the BGK model in Sec. II.

Equations (35)–(37) are the defining equations of spin hydrodynamics. We note that the equations indeed close. There are eight variables $n_\uparrow$,$n_\downarrow$,$\vec{u}_\uparrow$, and $\vec{u}_\downarrow$ and eight equations of motion. This is the case as long as we consider the temperature of the cloud to be fixed. If the evolution of T is needed then we can add an equation for the total energy density $\mathcal{E}$, see Eq. (28). We also note that if $\vec{u} \equiv \vec{u}_\uparrow = \vec{u}_\downarrow$ summing Eqs. (35)–(37) gives the usual Euler equation. If viscous effects are important, then we can either extend Eq. (33) to include an anisotropic temperature as in Ref. [6], or include a spin-independent term in Π^{ij}_σ, which is proportional to the viscous stresses.

V. DIFFUSIVE AND BALLISTIC LIMITS

In this section we will check that spin hydrodynamics does indeed correctly reproduce the diffusive and ballistic limits. First consider the diffusive case. The difference of the continuity equations gives

$$\partial_0 M + \vec{\nabla}\cdot(M\vec{u} + n\vec{w}) = 0. \tag{41}$$

The first term in the spin current is the advection term $\vec{j}_M \sim M\vec{u}$. The second term, $\vec{j}_M \sim n\vec{w}$ can be computed using the difference of the spin stress equations. In the diffusive limit these equations can be solved order by order in the small parameter τT. At leading order, and ignoring external forces, we find $\vec{w} = -\frac{\tau T}{mn}\vec{\nabla}M + \vec{w}_a$. Here, $\vec{w}_a$ is an $O(\tau)$ correction to the advection term $M\vec{u}$. Neglecting this term, we get

$$\partial_0 M - \vec{\nabla}\cdot(D\vec{\nabla}M - \vec{u}M) = 0, \tag{42}$$

with $D = \tau T/m$, in agreement with the result in Sec. II. We can also study the effect of an external force. In hydrostatic equilibrium we neglect the time derivatives and velocity terms. We get

$$\frac{T\vec{\nabla}n_\sigma}{n_\sigma} = -\vec{\nabla}V_{\rm ext}, \tag{43}$$

which implies $n_\sigma(x) \sim \exp[-V_{\rm ext}(x)/T]$. We can use this relation to express $V_{\rm ext}$ in terms of the density when solving for the spin current $\vec{w}$. We get

$$n\vec{w} = -\frac{\tau T}{m}\left(\vec{\nabla}M - \frac{M}{n}\vec{\nabla}n\right), \tag{44}$$

in agreement with Eq. (10).

In the opposite limit, that of infinite collision time, we expect the spin hydrodynamic equations to agree with solutions of the ballistic Boltzmann equation. In a trap these solutions correspond to simple spin-sloshing modes. Consider

$$f_{p\sigma}(x,t) = n_0(x_\perp,p_\perp)\exp\left(-\frac{m\omega_z^2}{2T}[z - \bar{\sigma}\,z_0\cos(\omega t)]^2\right)$$
$$\times\ \exp\left(-\frac{1}{2mT}[p_z - \bar{\sigma}\,p_0\sin(\omega t)]^2\right) \tag{45}$$

with $\bar{\sigma} = \pm$ for $\sigma = \uparrow\downarrow$ and

$$n_0(x_\perp,p_\perp) = \exp\left(-\frac{m\omega_\perp^2 x_\perp^2}{2T} - \frac{p_\perp^2}{2mT}\right). \tag{46}$$

This distribution solves the ballistic Boltzmann equation in a trap if $\omega = \omega_z$ and $p_0 = z_0 m\omega_z$. We can compute the spin densities

$$n_\sigma = n_0\exp\left(-\frac{m\omega_z^2}{2T}[z - \sigma\,z_0\cos(\omega t)]^2\right) \tag{47}$$

and the spin velocity $\vec{u}_\sigma = \pm\vec{w}$ with $w_z = p_0/m = \omega_z z_0$. The spin stresses are given by

$$\Pi^{ij}_\sigma = mn_\sigma w^i w^j + n_\sigma T\delta^{ij}. \tag{48}$$

It is now straightforward to check that Eqs. (47)–(48) satisfy the spin continuity equations (35) and the spin Euler equation

$$\partial_0\left(mn_\sigma u^i_\sigma\right) + \vec{\nabla}_j\Pi^{ij}_\sigma = -mn_\sigma F^i. \tag{49}$$

It is then reasonable to assume that spin hydrodynamics can describe the transition between diffusion and spin oscillations in a trap.

VI. SIMULATING SPIN HYDRODYNAMICS

We have implemented spin hydrodynamics in close analogy with our implementation of viscous fluid dynamics [23] and anisotropic fluid dynamics [6] for cold atomic Fermi gases. The numerical code is based on the piecewise parabolic method (PPM) Strike (Lagrangian remap) method of Colella and Woodward [24], as implemented in the VH1 code developed by Blondin and Lufkin [25]. We solve the conservation laws using Lagrangian coordinates. The momentum equations can be written as

$$D_\sigma u^i_\sigma = -\frac{1}{\rho_\sigma}\vec{\nabla}^i P_\sigma \mp \frac{\rho_g}{\rho_\sigma\tau}w^i, \tag{50}$$

where $D_\sigma = \partial_0 + \vec{u}_\sigma\cdot\vec{\nabla}$ is the comoving derivative, $\rho_\sigma = mn_\sigma$ is the mass density, and $P_\sigma = n_\sigma T$ is the partial pressure of the spin state σ. After a Lagrangian time step

the hydrodynamic quantities are remapped onto a Eulerian grid. The spin current $\vec{j}_M = M\vec{u} + n\vec{w}$ can be compared to the expectation from Fick's law, $\vec{j}_M = M\vec{u} - D\vec{\nabla}M$, where $D = \tau T/m$.

We consider diffusion in an axially symmetric trapping potential $V(x) = \frac{1}{2}m\omega_i^2 x_i^2$ with $\omega_x = \omega_y = \omega_\perp$ and $\omega_z = \lambda\omega_\perp$. We introduce dimensionless variables for distance, time, and velocity based on the following system of units [23]

$$x_0 = (3N\lambda)^{1/6}\left(\frac{2}{3m\omega_\perp}\right)^{1/2}, \quad t_0 = \omega_\perp^{-1}, \quad u_0 = x_0\omega_\perp, \tag{51}$$

where $N = N_\uparrow + N_\downarrow$ is the total number of particles. The unit of density is $n_0 = x_0^{-3}$, and the unit of temperature is $T_0 = m\omega_\perp^2 x_0^2$. Finally, the unit of the diffusion constant in

$$D_0 = \omega_\perp x_0^2. \tag{52}$$

We will use an overbar to denote dimensionless quantities, for example $\bar{x} = x/x_0, \bar{T} = T/T_0$, and $\bar{D} = D/D_0$.

In the high-temperature limit the initial density is a Gaussian. The density is

$$n(x) = n(0)\exp\left(-\frac{E_F}{E_0}[\bar{x}^2 + \bar{y}^2 + \lambda^2\bar{z}^2]\right), \tag{53}$$

where $\bar{x} = x/x_0$ is the dimensionless position, $E_F = (3N\lambda)^{1/3}\omega_\perp$ is the Fermi energy in the trap, and E_0 is the total energy per particle of the trapped gas. For an ideal gas $E_0 = 3NT$, and the dimensionless temperature is $\bar{T} = \frac{1}{2}(E_0/E_F)$. The central density is given by

$$n(0) = n_0\frac{N\lambda}{\pi^{3/2}}\left(\frac{E_F}{E_0}\right)^{3/2}. \tag{54}$$

It is convenient to normalize the central density to one,[1] so that $\bar{n} = n/n(0)$ and $\bar{M} = M/n(0)$.

A simple parametrization of the diffusion constant can be given in terms of a density-independent part, reflecting the low-temperature (quantum) behavior, and a part that scales inversely with density, corresponding to the high-temperature (kinetic) limit. We write

$$D = \frac{\beta}{m} + \frac{\beta_T}{m}\frac{(mT)^{3/2}}{n}, \tag{55}$$

where β and β_T are constants. The kinetic theory result given in Eq. (11) corresponds to $\beta_T = 3/(16\sqrt{\pi})$. In dimensionless units this formula becomes

$$\bar{D} = \bar{\beta} + \bar{\beta}_T\frac{\bar{T}^{3/2}}{\bar{n}}, \tag{56}$$

where $\bar{D} = D/D_0$ and

$$\bar{\beta} = \frac{3}{2}\frac{\beta}{(3\lambda N)^{1/3}}, \quad \bar{\beta}_T = \frac{4\pi^{3/2}}{3}\frac{\beta_T}{(3\lambda N)^{1/3}}\left(\frac{E_0}{E_F}\right)^{3/2}. \tag{57}$$

[1] In this work we will focus on the high-temperature limit, so that the equilibrium density is a Gaussian. We note, however, that the choice of units $\bar{n} = n/n_{id}(0)$, where $n_{id}(0)$ is the central density of the ideal gas at the same temperature is convenient also for a general equation of state.

Using these parameters we can provide some simple estimates for the time scales involved in simulations of diffusion in a trapped atomic gas. We saw that empirically the spin decay rate scales as $\Gamma = \omega_z^2/(\gamma E_F)(T/T_F)^{1/2}$, see the discussion preceding Eq. (17). The experiment of Sommer *et al.* gives $\gamma \simeq 0.16$. Based on the units described above the dimensionless decay time is

$$\bar{\Gamma}^{-1} = 2.87\gamma\frac{(\lambda N)^{1/3}}{\lambda}\left(\frac{E_F}{E_0}\right)^2, \tag{58}$$

where $\bar{\Gamma} = \Gamma/\omega_\perp$. Sommer *et al.* do not provide the precise values of λ and N in their experiment, but typical values used in the viscosity measurements reported in Refs. [26,27] are $N = 2\times10^5$ and $\lambda = 0.045$. These parameters lead to long decay times $\bar{\Gamma}^{-1} \simeq 212(E_F/E_0)^2$.

This estimate should be compared to the typical time step in a spin hydrodynamic simulation. In ordinary fluid dynamics the time step is controlled by the speed of sound and the resolution, $\Delta t = C\Delta x/c_s$, where the Courant number C is typically chosen to be 1/2. Using dimensionless units and the speed of sound of an ideal gas we find

$$\Delta\bar{t} = C\sqrt{\frac{6}{5}}\left(\frac{E_F}{E_0}\right)^{1/2}\Delta\bar{x}. \tag{59}$$

The units are chosen such that the cloud size is of order 1. Then $\Delta\bar{t} \lesssim \Delta x \lesssim 0.1$ is a typical time step for the hydrodynamic evolution. In spin fluid dynamics we also have to ensure that the time step is small compared to the relaxation time. The dimensionless relaxation time is

$$\bar{\tau} = \frac{\bar{\beta}}{\bar{T}} + \frac{\bar{\beta}_T\bar{T}^{1/2}}{\bar{n}}. \tag{60}$$

Using the estimate $\beta_T = 3/(16\sqrt{\pi})$ together with Eq. (57), as well as the values of N and λ given above, we get $\bar{\tau}(0) = 0.02(E_0/E_F)^2$. This suggests that for small λ and typical values of E_0/E_F there is a significant disparity of scales between the diffusive scale Eq. (58) and the relaxation scale Eq. (60). As a result, in the limit that the cloud is very deformed ($\lambda \to 0$) and the diffusion constant is very small ($\bar{\beta} \to 0$), spin hydrodynamics is potentially an inefficient method for simulating the diffusion equation. This is not necessarily a problem. First, if the diffusion constant is small diffusive behavior sets in quickly and the decay constant can be accurately determined even if the simulation time is less that Γ^{-1}. Second, a similar disparity of scales appears in the anisotropic hydrodynamics method as the shear viscosity becomes small. Anisotropic hydrodynamics is indeed an inefficient method for solving the Euler equation, but a powerful tool to extract the shear viscosity for realistic geometries [7].

VII. NUMERICAL RESULTS: BOX

In order to test spin hydrodynamics we have solved the equations of motion in a three-dimensional box. The simulation is carried out on a three-dimensional Cartesian grid with 50^3 points and a grid spacing $\Delta\bar{x} = 0.2$. We consider a constant background density $\bar{n}_\uparrow = \bar{n}_\downarrow = 1/2$ with a Gaussian perturbation $\delta\bar{n}_{\uparrow\downarrow} = \pm0.05\exp(-\bar{x}_i^2)$. The left panel in Fig. 2

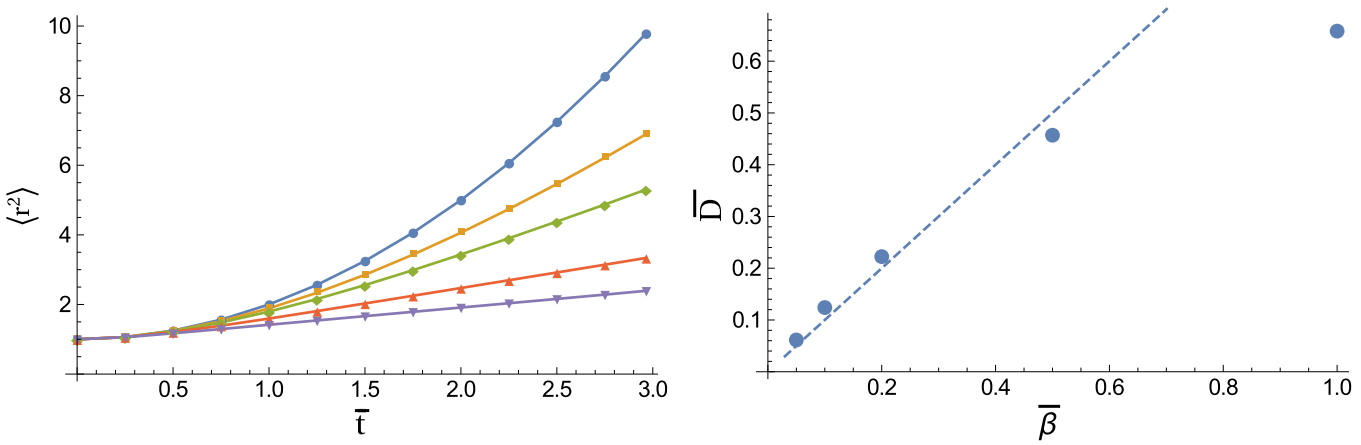

FIG. 2. The left panel shows the mean-square size $\langle r^2\rangle$ of the magnetization $M = n_\uparrow - n_\downarrow$ as a function of time for the evolution of a Gaussian initial state. The different curves correspond to different values of the diffusion parameter, from top to bottom $\bar{\beta} = (1000, 1, 0.5, 0.2, 0.1)$. We observe the transition from free expansion, $\langle r^2\rangle \sim \bar{t}^2$, to diffusion, $\langle r^2\rangle \sim \bar{t}$. The right panel shows the diffusion constant extracted from the growth of $\langle r^2\rangle$. The dashed curve shows the theoretical expectation in the small $\bar{\beta}$ limit.

shows the evolution of the mean-square magnetization radius

$$\langle r^2\rangle = \frac{1}{M_{\rm tot}} \int d^3\bar{x}\, \bar{x}_i^2 M(\bar{x},\bar{t}) \tag{61}$$

as a function of time. Here, $M_{\rm tot}$ is the integrated magnetization. The plot shows the result for a range of values of $\bar{\beta}$, corresponding to a range of relaxation times. We note that in a box, in which the background density is constant, there is no difference between the scaling with $\bar{\beta}$ and $\bar{\beta}_T$. In the limit of large $\bar{\beta}$ the squared radius grows quadratically with time, corresponding to a constant spin velocity $\vec{w}$ and ballistic expansion. For small values of $\bar{\beta}$ the squared radius grows linear with time, as expected from the solution of the diffusion equation. The diffusion equation predicts

$$M(\bar{x},\bar{t}) = \frac{M_0}{(1+4\bar{D}\bar{t})^{3/2}} \exp\left(-\frac{\bar{x}^2}{1+4\bar{D}\bar{t}}\right). \tag{62}$$

In the right panel of Fig. 2 we show the diffusion constant extracted from the slope of $\langle r^2\rangle$ together with the theoretical expectation $\bar{D} = \bar{\beta}$. The agreement for small $\bar{\beta}$ is quite good. In this regime there is a systematic shift between $\bar{\beta}$ and the extracted value of D, which indicates some amount of numerical diffusion.

In Fig. 3 we show the evolution of the magnetization in more detail. The left panel of Fig. 3 demonstrates that for large $\bar{\beta}$ (large relaxation time) the evolution is not diffusive. There is a magnetization front, which propagates at approximately constant speed. For small $\bar{\beta}$ (small relaxation time), on the other hand, the evolution is consistent with diffusion. This is seen more clearly in the right panel of Fig. 3, in which we compare the time and spatial dependence of the magnetization in spin hydrodynamics with the prediction from the diffusion law in Eq. (62).

In Fig. 4 we compare the spin current j_M in spin hydrodynamics with the expectation from Fick's law, $\vec{j}_M = -D\vec{\nabla}M$. Note that in the present case there is no convective contribution $M\vec{u}$. Fick's law predicts that the spin current turns on instantaneously, and then decays slowly as the cloud

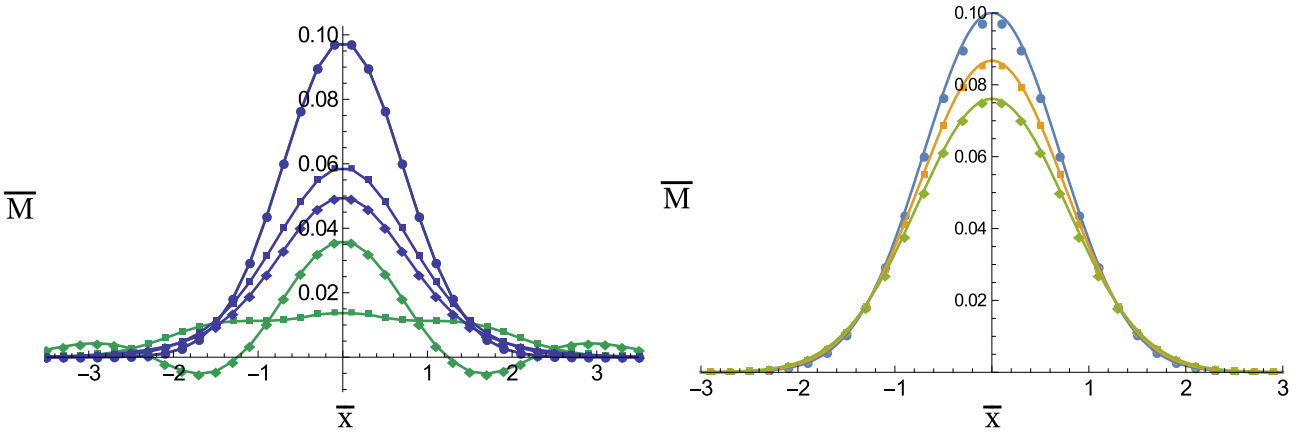

FIG. 3. The left panel shows the time evolution of the dimensionless magnetization $\bar{M}(\bar{x},\bar{t})$ for two different values of $\bar{\beta} = 1000$ (green diamonds) and $\bar{\beta} = 0.1$ (blue circles). The curves at $\bar{t} = 0$ (top) are identical, and only the $\bar{\beta} = 0.1$ graph is visible. The time step between successive curves is $\Delta\bar{t} = 1.25$. The right panel shows the time evolution of $M(\bar{x},\bar{t})$ for a small value of $\bar{\beta} = 0.05$. The dots show the result of spin hydrodynamics at different time steps separated by $\Delta\bar{t} = 0.5$ (time increasing from top to bottom), and the lines are the expectations from the diffusion equation (62).

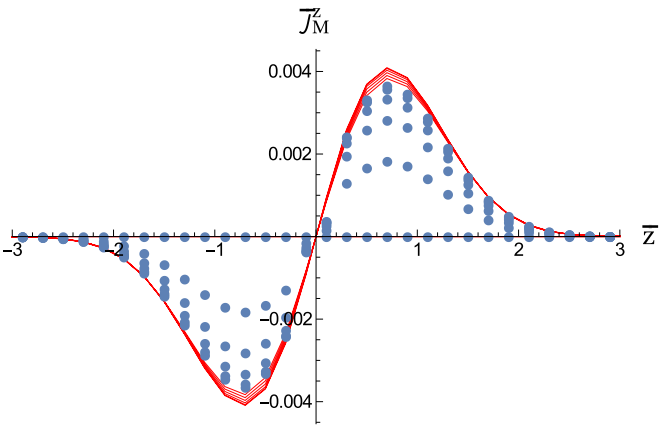

FIG. 4. Spin current $\vec{j}_M = n\vec{w} + M\vec{u}$ in spin hydrodynamics (dots) compared to the expectation from Fick's law, $\vec{j}_M = -D\vec{\nabla}M$ (lines). We show the z component of the dimensionless current as a function of $\bar{z}$ (with $\bar{x} = \bar{y} = 0$) for $\bar{\beta} = 0.05$ and several values of $\bar{t} = (0,0.05,0.10,0.15,0.20)$. Note that the prediction from Fick's law starts maximal and then decays (very slowly, on the time scale shown in this figure), whereas the current in spin hydrodynamics starts at zero and the approaches Fick's law.

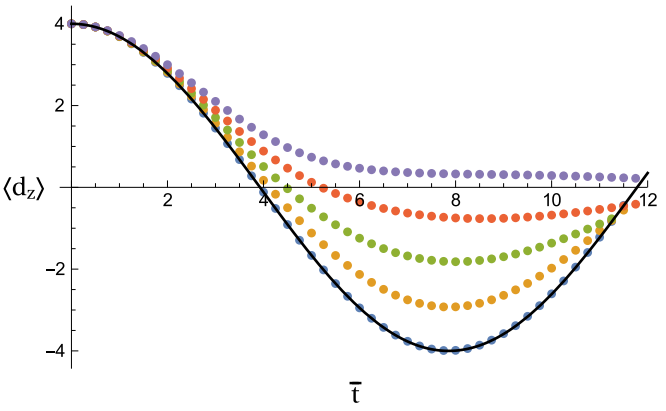

FIG. 5. Evolution of the spin dipole moment in a trapped gas a function of time. The initial condition is given by two shifted Gaussians, see Eq. (64). The solid line shows an undamped spin oscillation with frequency $\bar{\omega} = 0.4$. The points show the results of a spin hydrodynamics simulation with $\bar{\beta} = (1000,5,2,1,0.5)$, going from oscillatory to overdamped behavior.

expands. Spin hydrodynamics, on the other hand, predicts that the spin current vanishes at $\bar{t} = 0$ and then approaches Fick's law on a time scale set by the relaxation time. At late time the spin hydrodynamics current tracks Fick's law.

VIII. NUMERICAL RESULTS: TRAPPED GAS

In this section we will consider a harmonically trapped gas. We assume axial symmetry, and the simulations are carried out in cylindrical coordinates on a grid with dimensions 50^2 and grid spacing $\Delta\bar{z} = 0.2$ and $\Delta\bar{\rho} = 0.2$. The main observable is the spin dipole moment

$$d_z = \frac{2}{N_{\rm tot}} \int d^3\bar{x}\, \bar{z}\, M(\bar{x},\bar{t}), \tag{63}$$

which is the same quantity that was studied in the experimental work of Sommer *et al.* [9]. We first consider a density-independent relaxation time, governed by the parameter $\bar{\beta}$. The initial spin density is given by two shifted Gaussians

$$\bar{n}_\sigma = \frac{1}{2} \exp\left(-\frac{E_F}{E_0}[\lambda^2(\bar{z} \pm \bar{z}_0)^2 + \bar{\rho}^2]\right). \tag{64}$$

We use $E_0/E_F = 1, \lambda = 0.4$ and $\bar{z}_0 = 2$. For $\bar{\beta} \to \infty$ we expect the system to show undamped spin oscillations with frequency $\bar{\omega} = \lambda$, as described in Sec. V. This can be seen in Fig. 5. For finite but large $\bar{\beta}$ the gas exhibits damped oscillations, and for small β the motion is overdamped.

More details are shown in Fig. 6. The left and right panels show the evolution of the magnetization for $\bar{\beta} = 1000$ and $\bar{\beta} = 1$, respectively. We observe that for $\bar{\beta} = 1000$ the magnetization oscillates, and for $\bar{\beta} = 1$ it is strictly decaying. The decay is not precisely exponential, because the decay of the magnetization is superimposed on an undamped quadrupole oscillation of the total density. Physically, this mode is damped by shear viscosity, but we have not included viscosity in our study. Another possibility is to consider initial conditions that correspond to the late time dynamics of the trapped gas, and for which the total density is equilibrated. We choose

$$\bar{n}_\sigma = \frac{1}{2}\left(1 \pm A\frac{\bar{z}}{1+\lambda^2\bar{z}^2+\bar{\rho}^2}\right) \exp\left(-\frac{E_F}{E_0}[\lambda^2\bar{z}^2 + \bar{\rho}^2]\right), \tag{65}$$

which is motivated by the variational results derived in Sec. III.

The evolution of the spin dipole moment is shown in Fig. 7. The left panel demonstrates that the decay of the dipole moment is indeed exponential. The right panel shows the dependence of the decay constant on $\bar{\beta}$. For small $\bar{\beta}$ we observe a linear relationship. This behavior can be compared with the solution of the diffusion equation obtained in Sec. III. We obtained $\Gamma = \frac{D_0}{l_z^2}\Gamma_{\rm red}$ with $\Gamma_{\rm red} = 2$. In dimensionless units this can be written as

$$\bar{\Gamma} = \frac{1}{2\bar{T}}\,\bar{\beta}\lambda^2\,\Gamma_{\rm red}. \tag{66}$$

This relation is shown as the dashed line in the right panel of Fig. 7. We observe that $\Gamma_{\rm red} = 2$ indeed provides a very good description of the data for $\bar{\beta} \lesssim 0.5$. We conclude that spin hydrodynamics indeed converges to the expected solution of the diffusion equation in a trapped geometry.

We are now in a position to study the problem that motivated this study. Consider a diffusion constant that is inversely proportional to density, governed by the parameter $\bar{\beta}_T$ in Eqs. (55) and (56). We study the evolution in a deformed trap, beginning from the initial condition given in Eq. (65). As explained in Sec. III the diffusion equation predicts that for fixed diffusion constant D_0 at the trap center the decay of the spin polarization is much faster. This effect is caused by a large spin current in the dilute regime. In spin hydrodynamics, on the other hand, the relaxation time in the dilute regime is large, and we do not expect a large spin current to develop.

The time evolution of the spin dipole moment for different values of $\bar{\beta}_T$ is shown in the left panel of Fig. 8. We observe that for $\beta_T \lesssim 0.2$ the decay of the spin polarization is exponential. The extracted spin decay constant is shown in the right panel

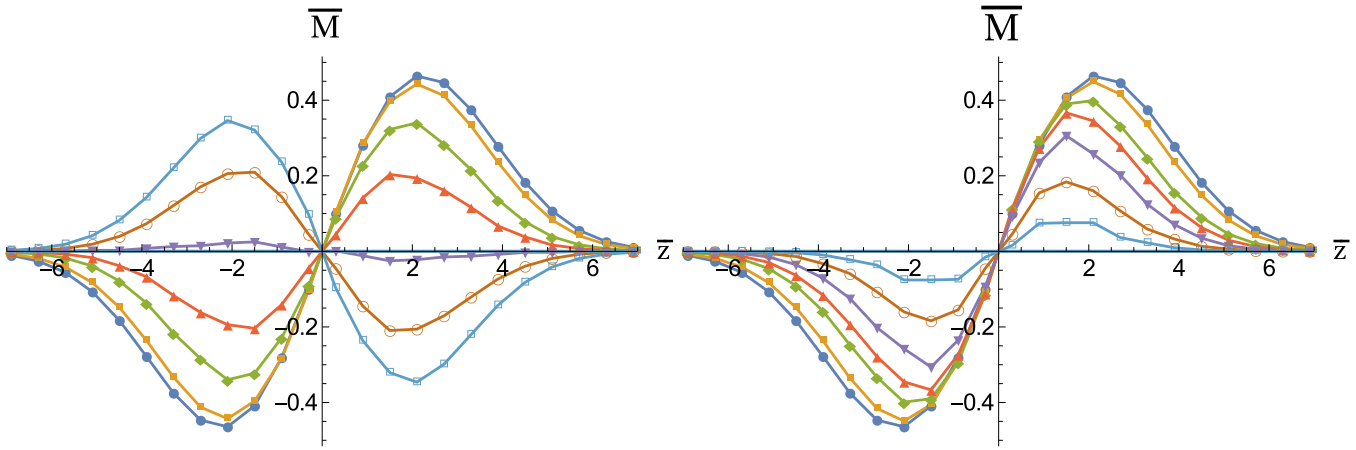

FIG. 6. Magnetization as a function of position for a trapped Fermi gas. The left panel shows the magnetization for different times in the ballistic (spin oscillation) limit $\bar{\beta} = 1000$. The curves are separated by $\Delta\bar{t} = 1.25$, starting with $\bar{t} = 0$ (blue circles). The right panel shows the magnetization at different times for $\bar{\beta} = 1$, closer to the diffusive limit.

of Fig. 8. As before, we can compare the result to solutions of the diffusion equation. In dimensionless units we get

$$\bar{\Gamma} = \frac{1}{2\bar{T}}\,\bar{\beta}\lambda^2\bar{T}^{3/2}\,\Gamma_{\rm red}. \tag{67}$$

We found that the diffusion equation predicts $\Gamma_{\rm red}(0.4) = 22.9$, whereas the experiment of Sommer *et al.* [9] indicates that $\Gamma_{\rm red} = 11.3$. Note that this result assumes the validity of kinetic theory, in particular the relation $D(0) = 0.106(mT)^{3/2}/[mn(0)]$, see Eq. (11). In spin hydrodynamics we can extract $\Gamma_{\rm red}$ from the slope of the $\bar{\beta}_T - \bar{\Gamma}$ relation. The dashed line in the right panel of Fig. 8 corresponds to $\Gamma_{\rm red} = 11$, and the error band indicates that the uncertainty in this analysis is about 10%. We can therefore deduce that

$$D(0) = (0.1 \pm 0.01)\frac{(mT)^{3/2}}{mn(0)}. \tag{68}$$

As a consistency check we have studied the dependence on the trap deformation λ. We have repeated the analysis shown in Fig. 8 for a smaller value $\lambda = 0.25$. We find smaller decay constants $\bar{\Gamma}$, and a slightly delayed onset of the linear behavior in the $\bar{\Gamma} - \bar{\beta}_T$ plot, but the reduced decay constant $\Gamma_{\rm red} = 11 \pm 1$ is unchanged. This is consistent with the experimental finding that the reduced decay constant does not depend on the trap deformation.

We note that the linear scaling with $\bar{\beta}_T$ implies that the damping constant is proportional to $\bar{T}^{3/2}E_0^{3/2} \sim T^3$. The first factor arises from the temperature dependence of the diffusion constant, and the second factor is due to the relation $T_F(0) \sim T^{-1}$ at fixed N and $\omega_\perp$,ω_z. The overall scaling of the damping constant contains an extra factor $l_z^{-2} \sim T^{-1}$, so that $\Gamma \sim T^2$. This is indeed the behavior observed in Ref. [9].

IX. CONCLUSIONS AND OUTLOOK

In this work we have derived the equations of spin hydrodynamics from an underlying kinetic theory. Spin hydrodynamics reduces to the diffusion equation in the dense limit, and to ballistic motion in the dilute limit. We have validated a numerical implementation of spin hydrodynamics using a

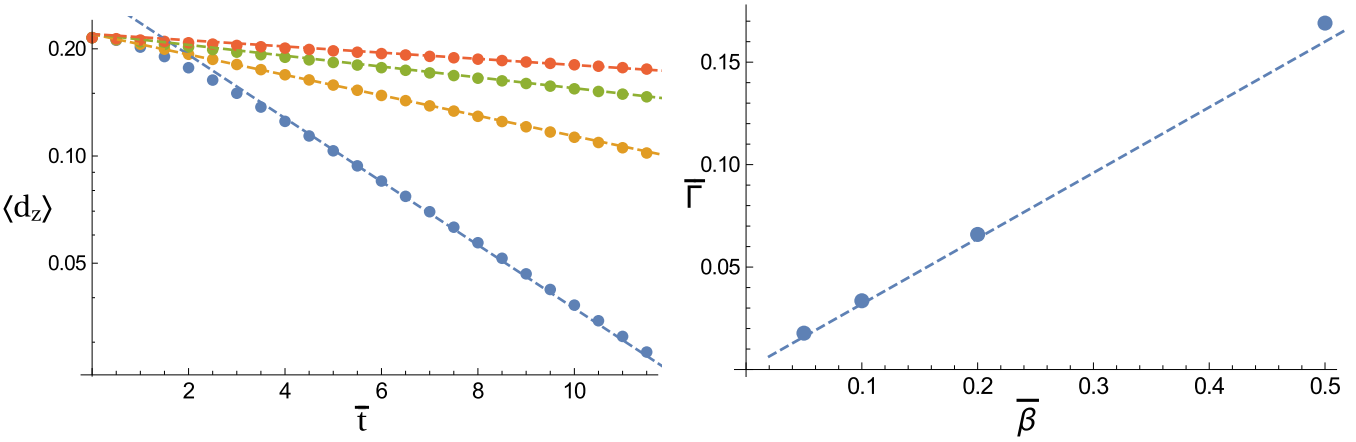

FIG. 7. The left panel shows the time evolution of the spin dipole moment in a trapped gas with a density-independent diffusion constant. The initial condition is given by Eq. (65). The points show the results of a spin hydrodynamics simulation with $\bar{\beta} = (0.5, 0.2, 0.1, 0.05)$, and the dashed lines are exponential fits. The right panel shows the extracted spin decay constant $\bar{\Gamma}$ as a function of $\bar{\beta}$. The dashed line corresponds to $\Gamma_{\rm red} = 2$ in Eq. (66).

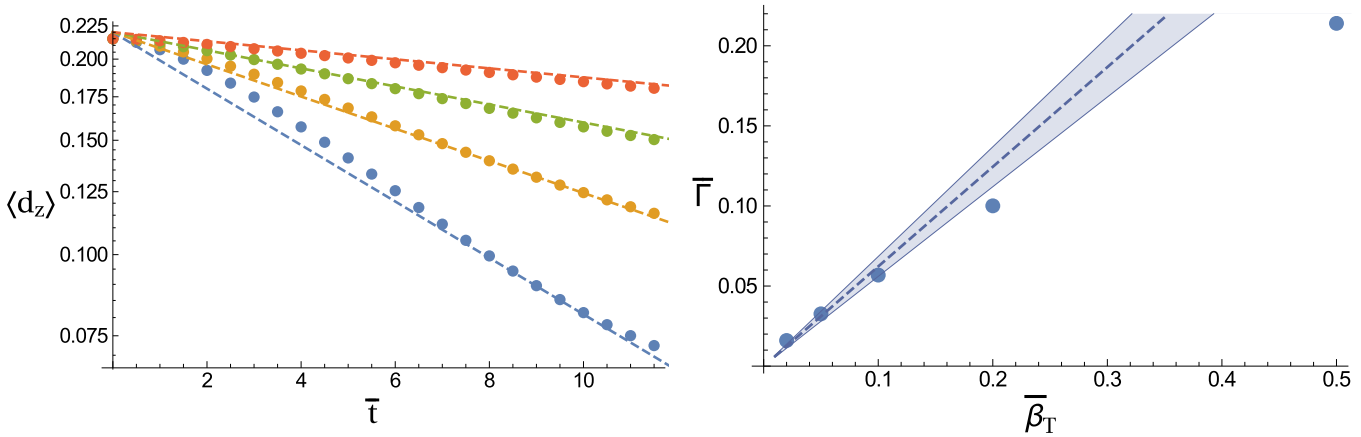

FIG. 8. The left panel shows the time evolution of the spin dipole moment in a trapped gas with $D \sim 1/n$. The initial condition is given by Eq. (65). The points show the results of a spin hydrodynamics simulation with $\bar{\beta}_T = (0.2, 0.1, 0.05, 0.02)$, and the dashed lines are exponential fits. The right panel shows the extracted spin decay constant $\bar{\Gamma}$ as a function of $\bar{\beta}$. The dashed line corresponds to $\Gamma_{\rm red} = 11$ in Eq. (67). The band shows a $\pm 10\%$ uncertainty in $\Gamma_{\rm red}$.

number of test cases. The diffusive limit was studied using the expansion of a Gaussian magnetization in a gas at constant density, and by following the decay of the spin dipole mode in a harmonic trap with density-independent diffusion constant. The ballistic limit was studied using the spin slosh mode in a harmonic trap.

We applied spin hydrodynamics to the decay of the spin dipole mode in a dilute Fermi gas at unitarity. In the high-temperature limit kinetic theory predicts that $D \sim T^{3/2}/n$. We verified that the experiment of Sommer *et al.* [9] is consistent with this prediction, and that the coefficient of proportionality agrees with kinetic theory. This conclusion was previously reached in the beautiful work of Bruun and Pethick [17], but these authors were forced to introduce an unknown parameter, the radial cutoff in the diffusion equation. Our method has no free parameters other than the diffusion constant. Sommer *et al.* concluded that agreement with kinetic theory can be achieved if the diffusion constant is corrected for the finite size of the trap.

A more detailed comparison to earlier work is shown in Fig. 9. The figure displays the profile of the spin current $\jmath_M$ and the spin velocity w in the transverse plane. We consider a diffusion constant of the form $D \sim T^{3/2}/n$, and we choose $\bar{\beta}_T = 0.05$. The left panel shows the spin current (dots) compared to the expectation from Fick's law (solid line) and the variational estimate discussed in Sec. III. We observe that the variational estimate is indeed close to Fick's law, but that the full spin current is significantly smaller than the variational result for $\bar{x} \gtrsim 2$. This is consistent with the conclusion of Bruun and Pethick that in order to match experimental data one has to impose a cutoff $r_0 \simeq 2.1 l_x$. The right panel shows the spin velocity at different times $\bar{t} = 0.25, 0.50, 0.75$. For comparison, we show the variational ansatz for the drift velocity $w_z \simeq w_z^0 (x/x_0)^2$ proposed by Sommer *et al.* [9], matched to fit the data. We observe that the agreement is very good in the regime $x \gtrsim l_x$, and that the data match the variational estimate out to larger distances as time progresses.

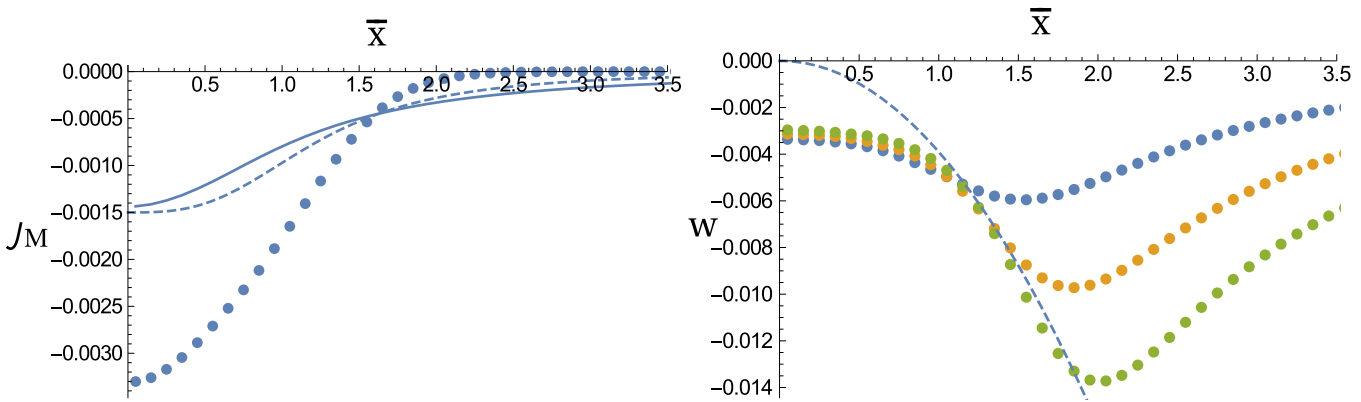

FIG. 9. Longitudinal spin current $\jmath_M$ (left) and spin velocity w (right) in the transverse plane. We show the z component of the current and the velocity at $\bar{z} = 0$ as a function of the transverse position $\bar{x}$ for $\bar{\beta}_T = 0.05$. The dots in the left panel show the spin current at $\bar{t} = 0.25$. The solid line is the expectation from Fick's law, and the dashed line is the variational estimate of the current profile obtained in Sec. III (scaled to fit Fick's law). The right panel shows the spin current at different times $\bar{t} = 0.25, 0.50, 0.75$ (top to bottom). The dashed line is the variational estimate of the drift velocity from Ref. [9], scaled to fit the data.

Our work can be extended in a number of ways. First, it is important to further test spin hydrodynamics using detailed comparisons with numerical simulations based on the Boltzmann equation in the weakly collisional limit. A similar study for anisotropic fluid dynamics is described in Refs. [7,28]. Second, we would like to perform precision determinations of the spin diffusion constant not only in the high-temperature limit, but also in the vicinity of the critical temperature for superfluidity. This will require implementing a more general functional form of the diffusion constant, and performing detailed fits of the temperature dependence of the decay rate of the spin dipole mode. The ultimate goal of this effort is to provide determinations of both the shear viscosity and the diffusion constant in the perfect fluid regime $a \to \infty$ and $T \sim T_c$, and to compare the results with expectations from quasiparticle theories as well as holographic models [29–31].

ACKNOWLEDGMENTS

This work was supported in parts by the US Department of Energy Grant No. DE-FG02-03ER41260. I would like to thank James Joseph and John Thomas for many useful discussions, and Georg Bruun and Martin Zwierlein for comments. I would also like to thank John Blondin for help with the VH1 code. This work was completed at the Institute for Nuclear Theory (INT) in Seattle during the program "The phases of dense matter".

[1] J. Crank, *The Mathematics of Diffusion*, 2nd ed. (Oxford University Press, Oxford, 1980).
[2] J. A. Pons, J. M. Ibáñez, and J. A. Miralles, Hyperbolic character of the angular moment equations of radiative transfer and numerical methods, Mon. Not. Roy. Astron. Soc. **317**, 550 (2000).
[3] E. O'Connor, An open-source neutrino radiation hydrodynamics code for core-collapse supernovae, Astrophys. J. Supp. Ser. **219**, 24 (2015).
[4] W. Florkowski and R. Ryblewski, Highly-anisotropic and strongly-dissipative hydrodynamics for early stages of relativistic heavy-ion collisions, Phys. Rev. C **83**, 034907 (2011).
[5] M. Martinez and M. Strickland, Dissipative dynamics of highly anisotropic systems, Nucl. Phys. A **848**, 183 (2010).
[6] M. Bluhm and T. Schäfer, Dissipative fluid dynamics for the dilute Fermi gas at unitarity: Anisotropic fluid dynamics, Phys. Rev. A **92**, 043602 (2015).
[7] M. Bluhm and T. Schäfer, Model-Independent Determination of the Shear Viscosity of a Trapped Unitary Fermi Gas: Application to High Temperature Data, Phys. Rev. Lett. **116**, 115301 (2016).
[8] J. Brewer, M. Mendoza, R. E. Young, and P. Romatschke, Lattice Boltzmann simulations of a strongly interacting two-dimensional Fermi gas, Phys. Rev. A **93**, 013618 (2016).
[9] A. Sommer, M. Ku, G. Roati, and M. W. Zwierlein, Universal spin transport in a strongly interacting Fermi gas, Nature (London) **472**, 201 (2011).
[10] M. Koschorreck, D. Pertot, E. Vogt, and M. Köhl, Universal spin dynamics in two-dimensional Fermi gases, Nat. Phys. **9**, 405 (2013).
[11] G. Valtolina, F. Scazza, A. Amico, A. Burchianti, A. Recati, T. Enss, M. Inguscio, M. Zaccanti, and G. Roati, arXiv:1605.07850 [cond-mat.quant-gas].
[12] X. Du, L. Luo, B. Clancy, and J. E. Thomas, Observation of Anomalous Spin Segregation in a Trapped Fermi Gas, Phys. Rev. Lett. **101**, 150401 (2008).
[13] X. Du, Y. Zhang, J. Petricka, and J. E. Thomas, Controlling Spin Current in a Trapped Fermi Gas, Phys. Rev. Lett. **103**, 010401 (2009).
[14] A. B. Bardon, S. Beattie, C. Luciuk, W. Cairncross, D. Fine, N. S. Cheng, G. J. A. Edge, E. Taylor, S. Zhang, S. Trotzky, and J. H. Thywissen, Transverse demagnetization dynamics of a unitary fermi gas, Science **344**, 722 (2014).
[15] S. Trotzky, S. Beattie, C. Luciuk, S. Smale, A. B. Bardon, T. Enss, E. Taylor, S. Zhang, and J. H. Thywissen, Observation of the Leggett-Rice Effect in a Unitary Fermi Gas, Phys. Rev. Lett. **114**, 015301 (2015).
[16] G. Bruun, Spin diffusion in fermi gases, New J. Phys. **13**, 035005 (2011).
[17] G. M. Bruun and C. J. Pethick, Spin Diffusion in Trapped Clouds of Strongly Interacting Cold Atoms, Phys. Rev. Lett. **107**, 255302 (2011).
[18] J. A. Joseph, E. Elliott, and J. E. Thomas, Shear Viscosity of a Universal Fermi Gas Near the Superfluid Phase Transition, Phys. Rev. Lett. **115**, 020401 (2015).
[19] T. Enss, C. Küppersbusch, and L. Fritz, Shear viscosity and spin diffusion in a two-dimensional Fermi gas, Phys. Rev. A **86**, 013617 (2012).
[20] T. Enss and R. Haussmann, Quantum Mechanical Limitations to Spin Diffusion in the Unitary Fermi Gas, Phys. Rev. Lett. **109**, 195303 (2012).
[21] T. Enss, Transverse spin diffusion in strongly interacting Fermi gases, Phys. Rev. A **88**, 033630 (2013).
[22] T. Enss, Nonlinear spin diffusion and spin rotation in a trapped Fermi gas, Phys. Rev. A **91**, 023614 (2015).
[23] T. Schäfer, Dissipative fluid dynamics for the dilute Fermi gas at unitarity: Free expansion and rotation, Phys. Rev. A **82**, 063629 (2010).
[24] P. Colella and P. R. Woodward, The Piecewise Parabolic Method (PPM) for Gas-Dynamical Simulations, J. Comp. Phys. **54**, 174 (1984).
[25] J. M. Blondin and E. A. Lufkin, The piecewise-parabolic method in curvilinear coordinates, Astrophys. J. Supp. Ser. **88**, 589 (1993).
[26] J. Kinast, A. Turlapov, and J. E. Thomas, Two Transitions in the Damping of a Unitary Fermi Gas, Phys. Rev. Lett. **94**, 170404 (2005).
[27] C. Cao, E. Elliott, J. Joseph, H. Wu, J. Petricka, T. Schäfer, and J. E. Thomas, Universal quantum viscosity in a unitary fermi gas, Science **331**, 58 (2011).
[28] P. A. Pantel, D. Davesne, and M. Urban, Numerical solution of the Boltzmann equation for trapped Fermi gases with in-medium effects, Phys. Rev. A **91**, 013627 (2015).
[29] T. Schäfer and D. Teaney, Nearly perfect fluidity: From cold atomic gases to hot quark gluon plasmas, Rep. Prog. Phys. **72**, 126001 (2009).

[30] H. Guo, D. Wulin, C.-C. Chien, and K. Levin, Perfect fluids and bad metals: Transport analogies between ultracold fermi gases and high T_c Superconductors, New J. Phys. **13**, 075011 (2011).

[31] A. Adams, L. D. Carr, T. Schäfer, P. Steinberg, and J. E. Thomas, Strongly correlated quantum fluids: Ultracold quantum gases, quantum chromodynamic plasmas, and holographic duality, New J. Phys. **14**, 115009 (2012).